

Computational Package for the Simulation of Plasma Microscopy Properties and Ion Beam-Plasma Interaction in High Energy Density Plasmas

†*Juan Miguel Gil^{1,2}, Rafael Rodríguez^{1,2}, Guadalupe Espinosa¹, and Pablo R. Beltrán¹

¹IUNAT, Departamento de Física, Universidad de Las Palmas de Gran Canaria, Spain.

²Instituto de Fusión Nuclear, Universidad Politécnica de Madrid, Spain.

*Presenting and †corresponding author: juanmiguel.gil@ulpgc.es

Abstract

Plasma microscopy properties and ion beam-plasma interaction are fundamental in many topics in plasma physics. Fundamental research and modelling in plasma atomic physics, like radiative properties and particle and laser beams-plasma interaction, continues to be essential for providing basic understanding and advancing on many different topics relevant to high-energy-density systems, particularly for nuclear fusion and astrophysics plasmas. In this work, we present a versatile computational package for the simulation and calculation of atomic and radiative properties of high energy density plasmas as well as the properties of ion-beam-plasma interaction processes. This computational package combines a set of theoretical and numerical approximations which yield substantial savings in computing running time, still comparing well with more elaborated codes and experimental data. Finally, calculations of several relevant plasma magnitudes for various plasma situations are shown and compared.

Keywords: Non-local thermodynamic equilibrium plasmas, Plasma atomic properties, Plasma radiative properties, Simulation and generation of databases of plasma properties, Ion beam-plasma interaction.

Introduction

Fundamental research and modelling in plasma atomic physics, like radiative properties and particle and laser beams-plasma interaction, continues to be essential for providing basic understanding and advancing on many different topics relevant to high-energy-density (HED) systems, particularly for nuclear fusion and astrophysics plasmas. Thus, in the field of inertial confinement fusion the radiative properties are the responsible of the absorption by the dopants in the fuel ablator of the thermal radiation in the indirect drive scheme. In magnetic confinement fusion devices, where the radiation emitted by the impurities could lead to thermal instabilities or to disruptions in the plasma edge. On the other hand, beam-matter interaction experiments are one of the key tools to investigate the fundamental physics properties of matter under extreme conditions, like high-energy-density plasmas, and a detailed theoretical description of the interactions allows us to diagnose the temperature and density, to obtain information about either the dynamic structure function or opacities and the equation of state of the plasmas. Also, the beam-matter interaction is one of the most essential problems in the nuclear fusion research area, in particular, in the field of beam-driven inertial confinement fusion, such as heavy-ion fusion or proton and ion fast ignition, where a precise knowledge of the energy deposition of the beam particles is required to design the fusion target. Therefore, the plasma properties are essential to analyze and explain both experiments and observations and also in their radiative-hydrodynamics numerical simulations. Furthermore, the simulations of the plasma properties in HED physics require the

development of complex theoretical models and their computational implementation for the generation of large plasma properties databases in a wide range of plasma conditions, as for example, atomic or opacity data. These plasma properties involve the calculation of a huge number of atomic levels (around 10^5) and atomic processes (around 10^7), by solving Dirac equations to obtain the atomic structure of each quantum atomic level of the ions considered in the plasma simulations, as well as, the cross sections of the atomic processes in the plasma. It is also necessary, to solve a very large set of coupled rate equations to obtain the average ionization of the plasma and the abundances of the atomic levels in both local thermodynamic equilibrium (LTE) and non-local thermodynamic equilibrium (NLTE) regimes. Moreover, this set must be solved for each plasma condition, i.e. density and temperature, the system must be resolved, and in a hydrodynamic simulation the profile of plasma conditions could involve around 10^3 of them.

In this work we present a versatile computational package based on three coupled codes named MIXKIP, RAPCAL [1-2] and STOPP, and their capabilities for the simulation of properties of the high energy density plasmas. MIXKIP code calculates the atomic structure and atomic kinetic of the ions in the plasma, RAPCAL code calculates the radiative properties and STOPP code calculates the energy losses of the ion beams crossing the plasma. This computational package combines a set of theoretical and numerical approximations which yield substantial savings in computing running time, still comparing well with more elaborated codes and experimental data. In order to show the capabilities of the package, calculations of several relevant plasma magnitudes for various plasma situations are shown and compared.

Theoretical and computational models

The determination of the atomic properties is the first step to be solved in the calculation of plasma properties in the HED plasmas. Our atomic model performs a detailed description (ion-by-ion) in the relativistic detailed configuration accounting approach (RDCA). So that each configuration i (either ground or excited one) of the ion with charge state ζ is characterized by one mono-electronic configuration, denoted by

$$C_{\zeta i} = \left\{ (c_{\zeta ik} \equiv nljm)_{k=1, \dots, N}^{w_{\zeta ik}} \right\}; \quad \sum_{k=1}^{M_{Z, \zeta}} w_{\zeta ik} = N_{\zeta} = Z - \zeta$$

where n , l , j , m are the principal quantum number, orbital momentum, total angular momentum and third component of the total angular momentum respectively; N_{ζ} is the number of bound electrons of the ion, $w_{\zeta ik}$ denotes the orbital occupation integer number, and finally, $M_{Z, \zeta}$ is the number of orbitals used in the representation of the configurations which is fixed depending on parameters like temperature, density, charge state or nuclear charge among others. For a given ion, for each relativistic configuration, we solve the Dirac equation for each occupied orbital which gives us its relativistic mono-electronic wave function. The corresponding energy is obtained using the density-functional theory (DFT) for each ion in the context of Kohn-Shan equations [3] and assuming the local density approach (LDA) for the exchange and correlation energy as well as for the exchange and correlation potential [4]. This scheme for isolated detailed atom has been extended for atoms and ions in plasmas (non-isolated ion), both for weakly and strongly coupled plasmas, where the external potential of the bound electron system is due to the nucleus of the ion and the plasma surrounding. The Dirac equation for each orbital k of the ion with atomic number Z , in the charge state ζ and excited state i -th is given by

$$[c\vec{\alpha} \cdot \vec{p} + c^2\beta + U_{ef,\zeta i}(r; Z, \bar{Z}(n, T))] \varphi_{\zeta ik}(\vec{r}) = \varepsilon_{\zeta ik} \varphi_{\zeta ik}(\vec{r})$$

where c is the light speed, α y β are the Dirac matrices, ε 's are the mono-electronic level energies and φ 's are the mono-electronic bi-spinor wave functions which depend on the major and minor component, P and Q respectively, which are given by

$$\varphi_{\zeta ik}(\vec{r}) \equiv \varphi_{nljm}(\vec{r}) = \frac{1}{r} \begin{pmatrix} P_{nlj}(r) \Omega_{ljm}(\theta, \phi) \\ iQ_{nlj}(r) \Omega_{l'jm}(\theta, \phi) \end{pmatrix}$$

being $l' = l \pm 1$ and Ω_{ljm} the spherical bi-spinors. Moreover, major and minor component can be obtained from coupled radial equations it is follows

$$\begin{aligned} \frac{dP_{nlj}}{dr} &= -\frac{\kappa}{r} P_{nlj} + \frac{1}{c} (\varepsilon_{nlj} - U_{ef,\zeta i}(r; Z, \bar{Z}(n, T))) Q_{nlj} \\ \frac{dQ_{nlj}}{dr} &= \frac{\kappa}{r} Q_{nlj} - \frac{1}{c} (\varepsilon_{nlj} - U_{ef,\zeta i}(r; Z, \bar{Z}(n, T)) - 2c^2) P_{nlj} \end{aligned}$$

with $\kappa = (l - j)(2j + 1)$. Finally, U_{ef} is the self-consistent non isolated effective potential which take into account the interaction of one bound electron with the nucleus of the ion, with the rest of bound electrons and the plasma surrounding. This effective potential depends on the atomic configuration and some plasma parameters, and for non-isolated ions in weakly coupled plasmas, we use the non-isolated atomic potential developed in [5], which is given by

$$U_{ef,\zeta i}(r; a) = -\frac{1}{r} \left\{ (N_\zeta - 1) (\Phi_{\zeta i}(r) - \eta_{\zeta i}(r; a)) + [Z - N_\zeta + (N_\zeta - 1)\eta_{\zeta i}(0; a)] e^{-ar} + 1 \right\}$$

with the screening functions of the non-hydrogenic ions given by

$$\Phi_{\zeta i}(r) = \frac{1}{(N_\zeta - 1)} \left\{ Z - N_\zeta + 1 - r \left[\sum_k w_{\zeta ik} \int \frac{|\varphi_{\zeta ik}(r')|^2}{|\vec{r} - \vec{r}'|} d\vec{r}' + U_{ex,\zeta i}(r) \right] \right\}$$

with

$$\rho_{\zeta ik}(r) \equiv |\varphi_{\zeta ik}(r)|^2 = \frac{1}{r^2} (P_{\zeta ik}(r) + Q_{\zeta ik}(r))^2$$

and

$$\eta_{\zeta i}(r) = \frac{1}{2} a \int_0^\infty e^{-a|s-r|} \rho_{\zeta i}(s) ds$$

being a the inverse of the Debye radius which depend on the electron density n_e and temperature T as well as on the average ionization \bar{Z} of the plasma, and is given by

$$a = \left[\frac{4\pi n_e (\bar{Z} + \bar{Z}^2)}{T \bar{Z}} \right]^{1/2}$$

For strongly coupled plasmas the non-isolated atomic potential used [6,7] is given by

$$U_{ef,\zeta i}(r; a) = -\frac{1}{r} (N_\zeta - 1) (\Phi_{\zeta i}(r) - \Phi_{\zeta i}(r; R_o)) + \frac{\bar{Z}}{2R_o} \left(1 - \frac{r^2}{R_o^2} \right)$$

at $r < R_o$ and $U_{ef,\zeta j}(r; a) = 0$ at $r > R_o$, being R_o the sphere-ion radius which is given by

$$R_o = \left[\frac{3\bar{Z}}{4\pi n_e} \right]^{1/3}$$

From the wave functions and level energies of all orbitals of each configuration, we calculate the relativistic configuration energy $E_{\zeta j}$, given by

$$E_{\zeta i}(r) = \sum_k w_{\zeta ik} \varepsilon_{\zeta ik} - \frac{1}{2} \sum_k w_{\zeta ik} \int |\varphi_{\zeta ik}(r')|^2 U_{\zeta i}(r) d\vec{r} d\vec{r}'$$

where $U_{\zeta i}(r)$ is the atomic potential due to the bound electrons of the ion, which can be obtained as $U_{\zeta i} = (Z/r) + U_{ef,\zeta i}(r; a = 0)$. Oscillator strength of the transition, from the mono-electronic orbital k to k' of the atomic configurations ζi and $\zeta i'$, respectively, is evaluated in the electric dipole approximation as it follows

$$f_{\zeta i, \zeta i'} = w_{\zeta ik} \left(1 - \frac{w_{\zeta i' k'}}{(2j' + 1)} \right) f_{\zeta ik, \zeta i' k'}$$

with

$$f_{\zeta ik, \zeta i' k'} = \frac{2}{3} (\varepsilon_{\zeta j' k'} - \varepsilon_{\zeta j k}) (2j' + 1) \times \\ \times \begin{pmatrix} j & 1 & j' \\ 1/2 & 0 & -1/2 \end{pmatrix} \left\{ \int_0^\infty [P_{\zeta ik}(r) P_{\zeta i' k'}(r) + Q_{\zeta ik}(r) Q_{\zeta i' k'}(r)] r dr \right\}$$

where $\begin{pmatrix} j_1 & j_2 & j_3 \\ m_1 & m_2 & m_3 \end{pmatrix}$ is the 3-j symbol. Another important magnitude overall in the interaction of particle beams with plasma is the mean excitation energy $I_{\zeta j}$ given by

$$\ln I_{\zeta i} = \frac{1}{N_{\zeta}} \sum_k w_{\zeta ik} \ln I_{\zeta ik}$$

where the mean excitation energy of each orbital is obtained as

$$I_{\zeta ik} = \sqrt{\frac{E_{c, \zeta ik}}{r_{\zeta ik}^2}}$$

being

$$E_{k, \zeta ik} = \varepsilon_{\zeta j k} - \int \varphi_{\zeta ik}^*(r) U_{ef, \zeta i}(r; Z, \bar{Z}(n, T)) \varphi_{\zeta ik}(r) d\vec{r}$$

and

$$r_{\zeta ik}^2 = \int \varphi_{\zeta ik}^*(r) r^2 \varphi_{\zeta ik}(r) d\vec{r}$$

Energies and oscillator strengths play a fundamental role in the photon absorption and emission processes from the plasma and in the spectral properties of the plasma, and mean excitation energies, in the energy deposition of ion beams in the plasmas.

Dirac equation is solved by a fourth order Runge-Kutta method in a linear or exponential radial mesh, and taking into account the semi-classical non-relativistic approximation at the origin and at practical infinity. There are many atomic equations (around 10^6) as configurations considered, and they are coupled with atomic rate equations by means of the average ionization of the plasma, and therefore, they must be solved iteratively. At high

temperature and low density, the effective potential tends to the isolated one, and the atomic and rate equations became uncoupled. On the other hand, although the number of atomic levels for a given isolated ion is infinite, this number should be finite for the atoms in a plasma if we want to obtain a satisfactory simulation of their radiative properties. This is due to the coulomb interaction between the bound electrons and the surrounding plasma, so we have to make a previous selection of the levels. However, there is not a priori criterion to determine which configurations should be included in the model. In general, the kind of configurations to include depends on the plasma conditions, the presence of external radiation fields or the interaction with particle beams. The experience achieved, based on the large number of cases studied during the development of the computational package, has led us to consider a complete enough set of configurations which allow us to obtain reasonable average ionization and ion abundances or populations. This set of configuration must be extended to obtain reasonable radiative properties of the plasma. In this case, the criterion employed was based on a rule of thumb in which the configurations included for each ion in the model are those with energies up to twice the ionization energy of the ground configuration of the ion. As said before, as the plasma density increase, screening effects due to neighbouring electrons and ions modify the atomic potential, and therefore, the ionization energy of the ground configuration. This effect is commonly modelled in plasma physics through the so-called continuum lowering, that represents the depression of the potential with respect to the isolated situation due to the electric fields generated by the plasma charged particles. This effect can restrict the number of configurations and, then, it determines the final set of atomic levels used for each plasma conditions. In this work, the model used for the continuum lowering is based on that provide by our self-consistent non isolated potentials, or based on the widely used one developed by Stewart and Pyatt [8]. Another question is related with the degree of detail of the atomic description. The most detailed description is the so-called detailed level accounting (DLA) approach. However, this description entails very large computational times and, therefore, it is only useful for chemical elements of low atomic number. This computational package has been designed to provide atomic data generated in the RDCA approach from low to high Z plasmas by solving the scheme explained before. Furthermore, this package has been also designed to work with external atomic data tables or codes. The current external atomic source is FAC code [9], which is designed to provide atomic data in DCA and DLA approaches.

Once the atomic data have been obtained, they are used in the second step which is the determination of the plasma level populations. The models commonly used for their calculation are based in the so-called collisional-radiative (CR) models [10], which are valid for plasmas either at LTE or NLTE. In these models, one has to solve a set of coupled atomic rate equations (one per each relativistic configuration in the present model) given by

$$\frac{dN_{\zeta i}(\mathbf{r}, t)}{dt} = \sum_{\zeta' i'} N_{\zeta' i'}(\mathbf{r}, t) \mathbb{R}_{\zeta' i' \rightarrow \zeta i}^+ - \sum_{\zeta' i'} N_{\zeta i}(\mathbf{r}, t) \mathbb{R}_{\zeta i \rightarrow \zeta' i'}^-$$

where $N_{\zeta i}$ is the population density of the atomic configuration or level i of the ion with charge state ζ . The terms $\mathbb{R}_{\zeta' i' \rightarrow \zeta i}^+$ and $\mathbb{R}_{\zeta i \rightarrow \zeta' i'}^-$ take into account all the atomic processes, both collisional and radiative, that contribute to populate and depopulate the configuration i of the ion ζ , respectively. Moreover, two complementary equations have to be satisfied together with the set of atomic rate equations. First, the conservation of the ion density n_{ion} ,

$$\sum_{\zeta=0}^Z \sum_{i=1}^{M_{Z,\zeta}} N_{\zeta i} = n_{ion}$$

and, second, the charge neutrality condition in the plasma,

$$\sum_{\zeta=0}^Z \sum_{i=1}^{M_{Z,\zeta}} \zeta N_{\zeta i} = n_e$$

In our computational package we solve the atomic rate equations for mono and multicomponent plasmas. For the last situation, we have also provide as an input data, the molar fractions of the chemical elements in the mixture which are given by $x_m = n_{ion,m}/n_{ion}$ and they have to be satisfied $\sum_m x_m = 1$, with m runs over the number of chemical elements in the plasma. The atomic processes included in the present CR model are: collisional ionization and three body recombination, spontaneous decay, collisional excitation and de-excitation, radiative recombination, electron capture and auto-ionization. The cross sections of these atomic processes in the plasma are calculated by mean of widely known analytical expressions [11] which depend on the atomic data calculated in the theoretical frame mentioned above. At this point we want to highlight that in the computational package are also implemented the Saha-Boltzmann and Coronal Equilibrium equations which provide the asymptotic behaviour of the atomic rate equations at high and low plasma electron density, respectively.

The rate coefficients of collisional processes between an ion, which goes from the state ζi to $\zeta' i'$, and one free electron, with incident energy ε , are obtained as

$$\langle v \sigma_{\zeta i \rightarrow \zeta' i'} \rangle = \int_{E_{th}}^{\infty} v \sigma_{\zeta i \rightarrow \zeta' i'}(\varepsilon) f(\varepsilon) d\varepsilon$$

where σ is the cross section of the processes, $v = \sqrt{2\varepsilon/m_e}$ and $f(\varepsilon)$ are, respectively, the speed and the distribution function of the free electrons. Free electron distribution function has to be solved from the free electron rate equation which is coupled with atomic rate equations. In our model, free electron plasma is assumed in LTE, and therefore, the free electron distribution function is given by the Boltzmann's distribution which is characterized by the plasma electron temperature. The rate coefficients of radiative processes between an ion, which goes from the state ζi to $\zeta' i'$, and one photon, with energy $h\nu$, are obtained as

$$\langle c \sigma_{\zeta i \rightarrow \zeta' i'} \rangle = \int_{E_{th}/h}^{\infty} c \sigma_{\zeta i \rightarrow \zeta' i'}(\nu) f_{ph}(\nu) d\nu$$

being f_{ph} the photon distribution function which is related with the spectral radiation intensity of the photons by mean $I_\nu = ch\nu f_{ph}(\nu)$. Radiative transfer equation provides the spectral radiation intensity from the following equation

$$\frac{1}{c} \frac{\partial I_\nu(\mathbf{r}, t, \nu, \mathbf{n})}{\partial t} + \mathbf{n} \cdot \nabla I_\nu(\mathbf{r}, t, \nu, \mathbf{n}) = -\kappa(\mathbf{r}, t, \nu) I_\nu(\mathbf{r}, t, \nu, \mathbf{n}) + j(\mathbf{r}, t, \nu)$$

where ν is the photon frequency, \mathbf{n} is a unit vector in the direction of propagation of the photons for any value of solid angle Ω , and finally, $j(\mathbf{r}, t, \nu)$ and $\kappa(\mathbf{r}, t, \nu)$ are the monochromatic emissivity and absorption coefficients, respectively. Both coefficients include electron transitions in the plasma between atom bound levels (line transitions or bound-bound contributions), between bound and free levels (photoionization and radiative recombination which are bound-free contributions) and between electron free levels (direct and inverse bremsstrahlung or free-free contributions). The expressions used to calculate them can be found elsewhere [12]. In our model, radiative transfer equation is assumed in stationary conditions, and therefore, the first sum in the left hand of the transfer equation equals zero. The formal solution of the radiative transfer equation, along the ray defined by the points of space (s_o, s) , is given by

$$I_\nu(s, \nu) = I_\nu(s_o, \nu)e^{\tau(s_o, s; \nu)} + \int_{s_o}^s j(s', \nu)e^{\tau(s', s; \nu)} ds'$$

being τ the optical depth, given by

$$\tau(s_o, s; \nu) = \int_{s_o}^s \kappa(s', \nu) ds'$$

Also, it is assumed a uniform distribution of emitting atoms and isotropic emission in the plasma in the three basic geometries (plane, cylindrical and spherical), and moreover, there are not external radiation fields. Then, spectral radiation intensity can be written as

$$I_\nu(s, \nu) = \frac{j(\nu)}{\kappa(\nu)} (1 - e^{-\kappa(\nu)(s-s_o)})$$

Two ingredients are needed to compute the spectral radiation intensity, or $j(\mathbf{r}, t, \nu)$ and $\kappa(\mathbf{r}, t, \nu)$. First, the cross sections of the radiative processes, which are obtained through atomic simulations. Secondly, the populations of the atomic levels in the plasma obtained from atomic rate equations. On the other hand, as the rate equations included the radiative processes in the plasma, i.e. spectral radiation intensity or the absorption and emissivity coefficients, one has to solve a set of coupled equations which are formed by atomic rate equations and radiative transfer equation. For optically thin plasmas, where the radiative processes can be despised in the atomic rate equations, the coupling is avoided and the atomic rate equations and radiative transfer equation can be solved separately: linear system of atomic rate equations are solved, and once the absorption and emissivity coefficients are obtained from atomic level populations, spectral radiation intensity is calculated. In the opposite case, for optically thick plasmas, the set of coupled equations are solved in the context of the escape factor formalism which avoids the explicit resolution of the radiative transfer equation. The formal solution of the transfer equation is introduced in the atomic rate equations, through rate coefficients of the bound-bound radiative processes, and now, a non-linear system of atomic rate equations is solved.

Another issue to consider is the method chosen for the solution of the atomic rate equations solver. When the electron density is taken as input parameter characterizing the population kinetics problem, then the set of rate equations constitute a linear system of M equations for the level populations, where M denotes the total number of levels included in the collisional-radiative model. Solvers can be broadly classified into two categories, direct and iterative. The direct solvers compute a solution which is guaranteed to be as accurate as the problem definition. The amount of time required to obtain a solution by such algorithms typically scale like M^3 . In a population kinetics problem, the number of levels can reach the order of 10^5 , so for such large systems of linear equation the direct methods lead to prohibitively long

run times. For the kind of problems that we are interested, the iterative methods yield an approximation to the solution significantly faster than direct method. Furthermore, iterative methods typically require less memory than direct ones and hence can be the only means of solution of the large systems of equations. Our code uses as initial population distribution the solution provided by either the corona model or the Saha-Boltzmann equations depending on whether the electron density of the case analysed is closer to the regime of low or high-density respectively.

Once the atomic data and plasma level populations the atomic configurations are obtained, by using the MIXKIP code, they are used as input data in RAPCAL code, to determine the radiative properties (spectrally resolved opacity and emissivity, specific intensity, mean Planck and Rosseland opacities or radiative power losses), or in the STOPP code to determine the energy deposition of the ion beams in plasmas (stopping power, energy losses or range). The basic equations of our radiative emissivity model to calculate $j(\mathbf{r}, t, \nu)$, has three contributions. The bound-bound contribution, $j_{bb}(\mathbf{r}, t, \nu)$, is given by

$$j_{bb}(\nu) = \sum_{\zeta} \sum_{i,j} j_{\zeta j \rightarrow \zeta i}(\nu), \quad j_{\zeta j \rightarrow \zeta i}(\nu) = \frac{h\nu}{4\pi} N_{\zeta j} A_{\zeta j \rightarrow \zeta i} N \phi_{ij}(\nu) \quad (14)$$

where we have omitted the dependence on the position and time in the formula for simplicity. $A_{\zeta j \rightarrow \zeta i}$ is the Einstein coefficient for spontaneous de-excitation between the bound states j, i of the ion ζ and h is the Planck's constant. $\phi_{ij}(\nu)$ is the line profile and in its evaluation of the line profile, natural, Doppler, and electron-impact [13] broadenings were included and also the Unresolved Transition Array width [14], which is a statistical method to take into account the atomic fine structure of the spectra in the DCA atomic approach used in this work. The line-shape function is applied with the Voigt profile that incorporates all these broadenings. The bound-free contribution to the emissivity, $j_{bf}(\mathbf{r}, t, \nu)$, is determined by means of

$$j_{bf}(\nu) = \sum_{\zeta+1,j} \sum_{\zeta,i} j_{\zeta+1,j \rightarrow \zeta,i}(\nu)$$

$$j_{\zeta+1,j \rightarrow \zeta,i}(\nu) = \frac{h^4 \nu^3 n_e}{2\pi c^2 \varepsilon_0^2} \left(\frac{1}{2m_e} \right)^{\frac{3}{2}} N_{\zeta+1,j} f(\varepsilon) \frac{g_{\zeta,i}}{g_{\zeta+1,j}} \sigma_{\zeta+1,j \rightarrow \zeta,i}^{\text{pho}}(\nu) \quad (15)$$

where ε is the free electron energy and m_e the electron mass. In this work, a Maxwell-Boltzmann distribution $f(\varepsilon)$ at the electron temperature is assumed. Photoionization cross section, $\sigma_{\zeta+1,j \rightarrow \zeta,i}^{\text{pho}}(\nu)$, were calculated quantum-mechanically using the FAC code in the relativistic distorted wave approach. $g_{\zeta,i}$ denotes the statistical weight of level i . Finally, for the free-free contribution to the emissivity a semi-classical expression, based on the Kramer's inverse bremsstrahlung cross section [15], was used

$$j_{ff}(\nu) = \frac{32\pi^2 e^4 a_0^2 \alpha^3}{\sqrt{3}(2\pi m_e)^{3/2} h} \left(\frac{m_e}{2\pi k_B T_e} \right)^{1/2} \frac{1}{Z^2} n_{\text{ion}} n_e e^{-h\nu/k_B T_e} \quad (16)$$

where k_B is the Boltzmann's constant and α is the fine structure constant.

Finally, we present the basic equations of the ion beam-plasma interaction model implemented in STOPP code, which allow us to determine the energy losses and the range of the ion beam from the stopping power. We consider two contributions to the total stopping power, both bound and free electrons. Bound contribution proposed is given by

$$S_b(v_p, Z, Z_p; n_{at}, T, \bar{Z}) = \frac{Z_p^2 e^4 n_{at}}{4\pi\epsilon_0^2 v_p^2} L_b$$

where the bound stopping number L_b is given by

$$L_b = \begin{cases} (Z - \bar{Z}) \left(\log \left(\frac{2m_e}{I} \right) - \frac{2E_k}{m_e v_p^2} \right), & \text{if } v_p > v_{int} \\ (Z - \bar{Z}) \left(\frac{\alpha v_p^3}{1 + G v_p^2} \right), & \text{if } v_p < v_{int} \end{cases}$$

where Z_p is the charge of the projectile, I and E_k are the mean excitation energy and mean kinetic energy of the bound electrons in the plasma, given by

$$I = \prod_{\zeta i} I_{\zeta i}^{p_{\zeta i} N_{\zeta i} / (Z - \bar{Z})}$$

and

$$E_k = (1/Z - \bar{Z}) \sum_{\zeta i} p_{\zeta i} E_{k, \zeta i}$$

being $p_{\zeta i}$ the normalized population density, α the viscosity coefficient of the bound electrons, given by

$$\alpha = 1.067 E_k^{1/2} I^2$$

and finally, G is a constant determined from the continuity condition of the bound stopping number at v_{int} , with $v_{int} = \sqrt{3E_k + 1.5I}$.

Free electron contribution to the total stopping power is given by [16]

$$S_e(v_p, Z, Z_p; n_e, T, \bar{Z}) = \frac{Z_p^2 e^4 n_e}{4\pi\epsilon_0^2 v_p^2} (G_e L_e + H_e \log X_e)$$

with the free stopping number given by

$$L_e = \log \left(\frac{R_D}{b} \right)$$

where R_D is the Debye radius, $b = Z_p e^2 / 4\pi\epsilon_0 m_e (v_p^2 + v_e^2)$ is the impact parameter, and v_e is the mean velocity of the free electrons. G_e and H_e functions are given by

$$G_e = \text{erf}(X_e / \sqrt{2}) - \sqrt{\frac{2}{\pi}} X_e e^{-X_e^2 / 2}$$

and

$$H_e = -\frac{X_e^3 \log X_e e^{-X_e^2 / 2}}{3\sqrt{2\pi}} + \frac{X_e^4}{(X_e^4 + 12)}$$

where X_e is the ratio between the projectile and free electron speeds. The ion-beam plasma interaction model implemented in STOPP code is valid to linear interaction regimen, non-degenerated free electrons, and finally, fast collisions.

Results

In this section we present some examples of the simulations carried out with the computational package based on the MIXKIP, RAPCAL and STOPP codes present before. First, we consider the spectral emission of shock waves in xenon plasmas doped with helium, at density and temperature conditions of the shock waves generated at PALS [17]. In Figure 1 we show the total emissivity and opacity, vs photon energy, of the mixture plasma with 90% of Xe and 10% of He, at matter density and electron temperature given by 1.5 gcm^{-3} and 10 eV , respectively. The spectral emissivity and opacity of the Xe and He as well as the total are showed, and we focus our attention in the experimental spectral window given by 35-80 eV. At this spectral energy, photons from Lyman series of the helium-like-hydrogen ion are present, and their characterization can be used to diagnose the electron density and temperature of the plasma. In

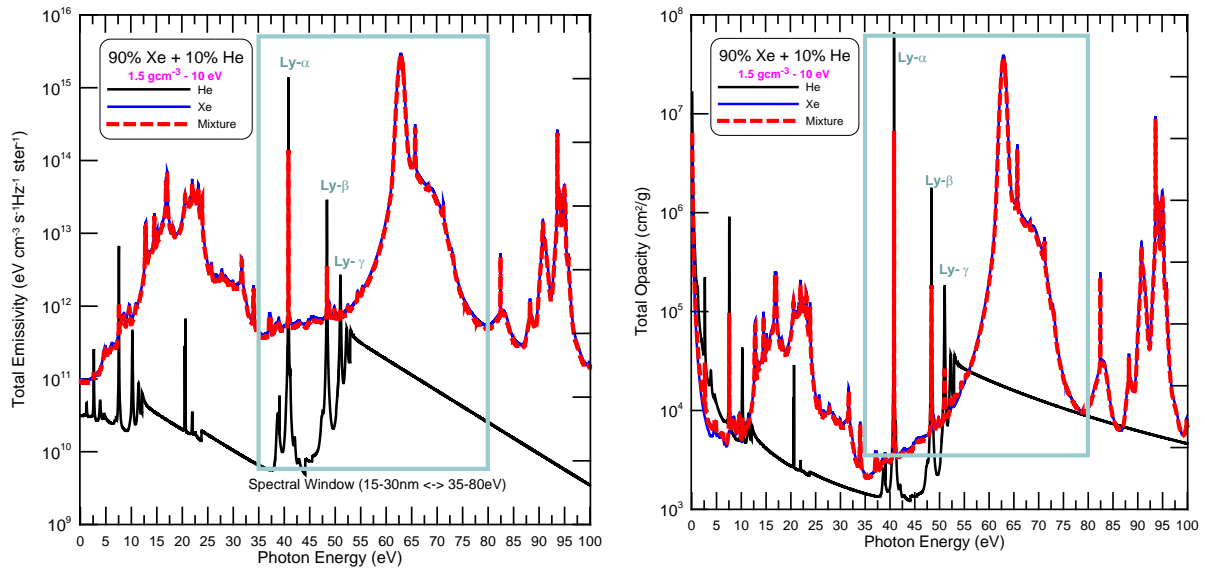


Figure 1. Spectral emissivity and opacity of Xe (90%) and He (10%) plasma mixture at 1.5 gcm^{-3} and 15 eV .

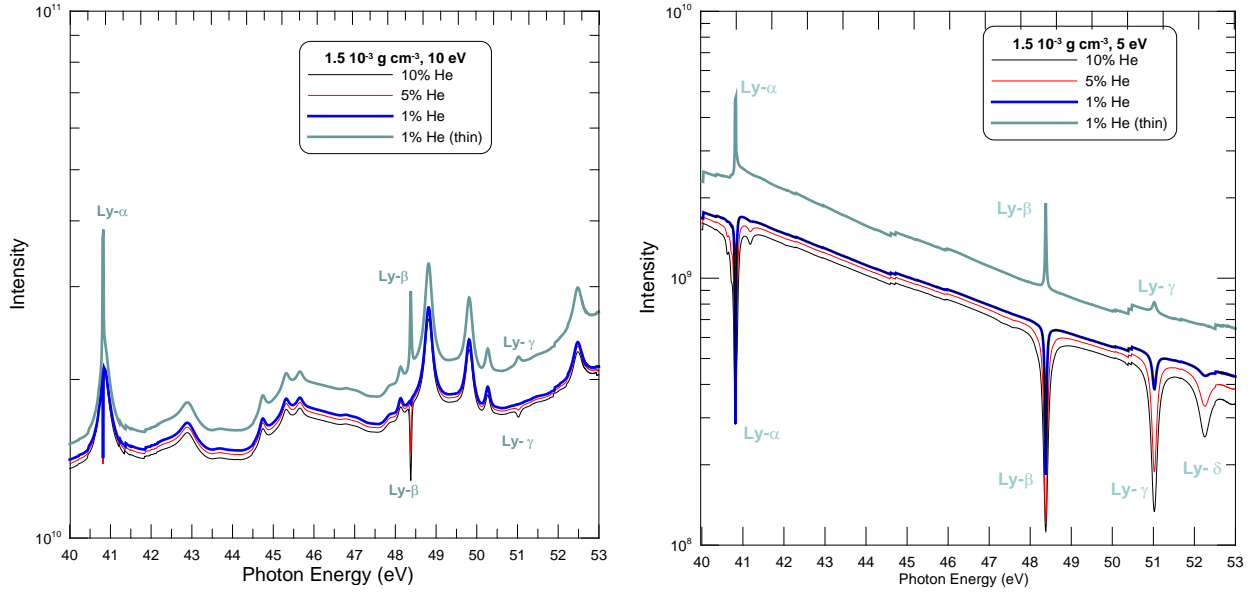


Figure 2. Specific radiative intensity emitted by Xe (90%) and He (10%) plasma mixture at 1.5 g cm^{-3} and 6 and 10 eV.

Figure 2 we show the specific radiative intensity emitted by a portion of plasma given by $0.6 \times 4 \times 0.025 \text{ mm}$, at matter density of 1.5 g cm^{-3} and temperatures of 5 and 10 eV, and finally, for different molar fractions of helium in the plasma. It can be observed that the intensity decrease when the temperature and molar fraction arise. It can also be observed the contribution to the total intensity of the Lyman series emitted from helium and the sensibility of the spectrum to the temperature.

In Figure 3 we show the stopping power and kinetic energy of proton beam at 0.5 MeV in aluminum plasma at 50 eV and different atom or ion densities, as function of depth in the plasma. It has been calculated by solving the atomic rate equation in the optically thin approximation and Saha-Boltzmann equations with the aim to simulate NLTE and LTE thermodynamic regimes in the plasma. At low densities, important differences in the stopping and kinetic energies of the proton are observed, while at high densities, NLTE and LTE simulations provide very similar results. The maximum stopping power calculated from atomic rate equations (NLTE) is lower than those obtained from Saha-Boltzmann equations (LTE) while the range is greater.

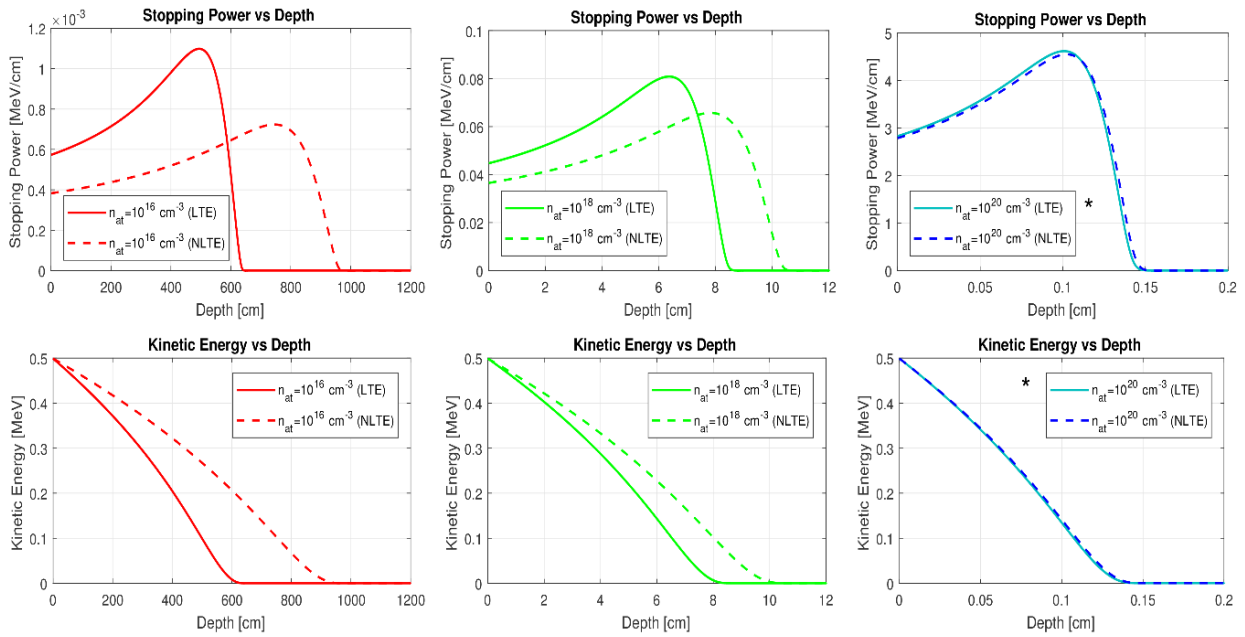


Figure 3. Stopping power and kinetic energy of proton beam at 0.5 MeV in aluminum plasma at 50 eV and different ion densities, as function of depth in the plasma.

Conclusions

In this work we have presented a versatile computational package designed to simulate plasma properties of the high energy density physics in a wide range of plasma conditions and combine a set of theoretical and numerical approximations which yield substantial savings in computing running time, still comparing well with more elaborated codes and experimental data. So, it can be simulated the atomic structure, atomic kinetic and radiative properties as well as the energy deposition of the ion beams in mono and multicomponent plasmas at LTE and NLTE thermodynamic regimens. It can also be simulated the properties of the optically thin and thick plasmas, and finally, of the non-stationary plasmas. These plasma properties involve the calculation of a huge number of atomic levels (around 10^5) and atomic processes (around 10^7), by solving Dirac equations to obtain the atomic structure of each quantum atomic configuration of the ions considered in the plasma simulations, as well as, the cross sections of the atomic processes in the plasma. It is also necessary, to solve a very large set of coupled rate equations to obtain the average ionization of the plasma and the abundances of the atomic configurations. Moreover, this set must be solved for each plasma condition, i.e. density and temperature, the system must be resolved, and in a hydrodynamic simulation the profile of plasma conditions could involve around 10^3 of them. Finally, calculations of several relevant plasma magnitudes for various plasma situations are shown and compared.

Acknowledgements

This work has been supported by the EUROfusion Consortium TASK AGREEMENT WPENR: Enabling Research IFE, Project No. AWP15-ENR-01/CEA-02, by the Project of the Spanish Government with reference FIS2016-81019-P.

References

- [1] Espinosa, G., Rodríguez, R., Gil, J.M., Suzuki-Vidal, F., Lebedev, S.V., Ciardi, A., Rubiano, J.G. and Martel, P. (2017) Influence of atomic kinetics in the simulation of plasma microscopic properties and thermal instabilities for radiative bow shock experiments, *Physical Review E* **95**, 033201.
- [2] Rodríguez, R., Florido, R., Gil, J.M., Rubiano, J.G., Suarez, D., Martel, P., Mínguez, E. and Mancini, R.C. (2010) Collisional-Radiative calculations of optically thin and thick plasmas using the computational package ABAKO/RAPCAL, *Communications in Computational Physics* **8**, 185-210.
- [3] Kohn, W. and Sham, L.J. (1965), *Physical Review A* **140**, 1133.
- [4] Gunnarsson, O. and Lundvist, B. (1976), *Physical Review B* **13**, 4274.
- [5] Gil, J.M., Martel, P., Mínguez, E., Rubiano, J., Rodríguez, R. and Ruano, F. (2002), *J. Quantum Spec. Radiat. Transfer* **75**, 539.
- [6] Gil, J.M., Martel, P., Rubiano, J., Rodríguez, R., Mínguez, E. and Doreste, L. (1997), in *Advances in laser interaction with matter and inertial fusion (World Scientific)*, pp. 335-338.
- [7] Rodríguez, R., Gil, J.M. and Florido, R. (2007), *Phys. Scr.* **76**, 418.
- [8] Stewart, J.C. and Pyatt, K.D. (1966) Lowering of ionization potentials in plasmas (1966), *The Astrophysical Journal* **144**, 1203-1211.
- [9] Gu, M.F. (2008) The flexible atomic code, *Canadian Journal of Physics* **86**, 675-689.
- [10] McWirther, R.W. P. (1978) Data needs, priorities and accuracies for plasma spectroscopy, *Physics Reports* **37**, 165-209.
- [11] Rodríguez, R., Florido, R., Gil, J.M., Rubiano, J.G., Martel, P. and Mínguez, E. (2008) RAPCAL code: A flexible package to compute radiative properties for optically thin and thick low and high-Z plasmas in a wide range of density and temperature, *Laser and Particle Beams*, 26, 433-448.
- [12] Rodríguez, R., Florido, R., Gil, J.M., Rubiano, J.G., Suarez, D., Martel, P., Mínguez, E. and Mancini, R.C. (2010) Collisional-Radiative calculations of optically thin and thick plasmas using the computational package ABAKO/RAPCAL, *Communications in Computational Physics* **8**, 185-210.
- [13] Dimitrijevic, M.S. and Konjevic, N. (1987) Simple estimates for Stark-broadening of ion lines in stellar plasmas, *Astronomy & Astrophysics* **172**, 345-349.
- [14] Bauche, J., Bauche-Arnoult, C. and Klapisch, M. (1987) Transition arrays in the spectra of ionized atoms, *Advance Atomic Molecular Physics* **23**, 131-195.
- [15] Rose, S.J. (1992) Calculation of the radiative opacity of laser-produced plasmas, *Journal of Physics B: Atomic and Molecular Physics* **25**, 1667-1681.
- [16] Thomas, P. and Meyer-ten-Vehn, J. (1991), *Phys. Rev. A* **43**,4.
- [17] Singh, R.L. et al. (2017), *High Energy Density Physics* **23**, 20-30.